Journal of
Chemical Engineering & Process Technology

Singh and Bansal, J Chem Eng Process Technol 2012, S1
DOI: 4172/2157-7048.S1-004

Research Article Open Access

Enhancement of Sieve Tray Efficiency using Computational Fluid Dynamics

Sumit Singh* and Ajay Bansal

Department of Chemical Engineering, Dr. B R Ambedkar National Institute of Technology, Jalandhar, India

Abstract

High degree of competitiveness associated with petroleum leads to the exhaustive search for new technologies that enable greater efficiency in the related processes. A three-dimensional mathematical homogeneous biphasic model was implemented in the commercial code of Computational Fluid Dynamics (CFD), FLUENT package to predict concentration and temperature distributions on sieve trays of distillation columns and good simulation results are obtained. The tray geometries and operating conditions are based on the experimental works of Indian oil corporation limited (R&D). The dispersed gas phase and continuous liquid phase are modelled in the mixture model for two interpenetrating phases with inter phase momentum, heat and mass transfer. The main objective of this study has been to find the extent to which CFD can be used as a prediction tool for real behaviour, and concentration and temperature distributions of sieve trays. The simulation results are shown that CFD is a powerful tool in tray design, analysis and trouble shooting, and can be considered as a new approach for efficiency calculations.

Keywords: Computational Fluid Dynamics (CFD); FLUENT; Distillation; Sieve tray

Introduction

Distillation is a separation process of major importance in the chemical industries, and known as the energy-intensive process. Distillation is the first choice for separation of liquid mixtures, the separation occur as a result of differences in the volatilities of the constituent components in the mixture being separated. Therefore, distillation involves simultaneous mass and heat transfer between the liquid and vapour phases. Sieve trays as the contacting device are widely used in distillation columns for their simplicity and low construction cost.

Tray design heavily relies on experience [1] because little is known about the flow behaviour and heat- and mass-transfer on the tray. The main reason for this is the poor understanding of the complex behaviours of the multiphase flow inside the tray. A good understanding of heat- and mass transfer and pressure drop fundamentals will enable the column designer effectively determine the optimal equipment design.

Current practice of tray design and analysis demonstrate that there are two major unresolved problems in analysis of tray hydrodynamics and performance.

1) The first one is what flow patterns to expect for given geometry and operating conditions.

2) To relate these flow patterns to tray performance parameters such as tray efficiency and pressure drop.

The description of the hydrodynamics of sieve trays is of great importance in industrial practice. For a given set of operating conditions (gas and liquid loads), tray geometry (column diameter, weir height, weir length, diameter of holes, fractional hole area, active bubbling area, down comer area) and system properties, it is required to predict the flow regime prevailing on the tray, liquid hold-up, clear liquid height, froth density, interfacial area, pressure drop, liquid entrainment, gas and liquid phase residence time distributions and the mass transfer coefficients in either liquid phase. There are excellent surveys of the published literature in this area [2-5] and published literature correlations are largely empirical in nature. In this paper a three-dimensional transient CFD model is developed, within the two-phase Eulerian framework, for hydrodynamics of a circular and rectangular tray. The required interphase momentum exchange coefficient is estimated on the basis of the correlation of Bennett et al. [1] for the liquid holdup. In this work a model is developed using CFD tool to give the predictions of the fluid flow patterns, and heat and mass transfer over sieve tray. The main objective has been to find the extent to which CFD can be used as a design and prediction tool for real behaviour, concentration and temperature distributions, and efficiencies of industrial trays.

Geometry

Fluent package of Ansys, Inc is used to model and simulate this problem. This package includes:

- Fluent ,the solver
- GAMBIT, the pre-processor for geometry modelling and mesh generation
- TGRID, an additional pre-processor that can generate volume meshes from existing boundary meshes.

System geometry: Based on trays specification [1], sieve trays, that is, both circular and rectangular are created in Gambit and boundary conditions are defined for system. Design is also created on ProE (Figure 1) for proper visualisation and solid or wireframe is exported to gambit. The dimensions of computational space are 260*233*233

***Corresponding author:** Sumit Singh, Department of Chemical Engineering, Dr. B R Ambedkar National Institute of Technology, Jalandhar, India, Tel: +91-7837053603; Fax: +91-0183-2587265; E-mail: sumit_nitj@yahoo.com

Received April 09, 2011; **Accepted** May 21, 2012; **Published** May 23, 2012

Citation: Singh S, Bansal A (2012) Enhancement of Sieve tray efficiency using Computational Fluid Dynamics. J Chem Eng Process Technol S1:004. doi:10.4172/2157-7048.S1-004

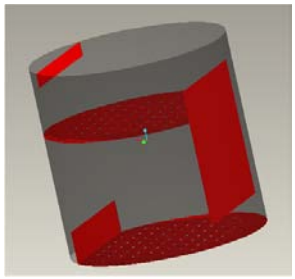

Figure 1: Showing the circular tray design in ProE.

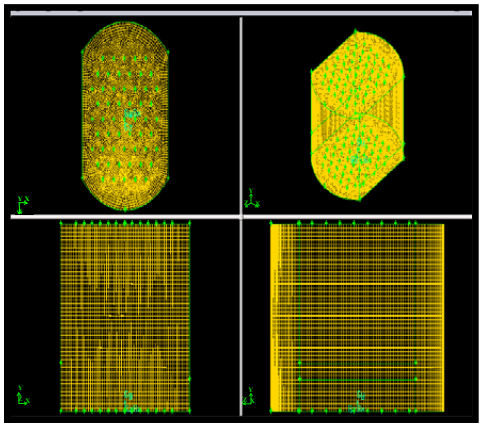

Figure 2: Showing the design of Tray in Gambit in all four views with meshing.

Case	Geometry	Mesh used	Results
1	Rectangular sieve tray	Cooper	Geometry created and Exported to CFD package
2	Circular sieve tray	Cooper	Geometry created and Exported to CFD package

Table 1: Type of Mesh Used.

mm as shown in Figure 2. Grid cells of 5 mm are used in the x, y and z directions. The chosen grid size of 5 mm is based on where convergence criteria. The total number of grid cells within the computational space are 239747 (Table 1).

Mathematical modelling

The model considers the gas and liquid flows [6,7] in a mixture model framework, where the phases are treated with transport equations. The equations used were continuity, momentum and energy equations. To solve these, it was necessary to add and use the equation of momentum flux. Following equations are used:

Continuity equation

Gas phase:

$$\frac{\partial(r_G\rho_G)}{\partial t}+\nabla.(r_G\rho_G V_G)+S_{LG}=0 \quad (1)$$

Liquid phase:

$$\frac{\partial(r_L\rho_L)}{\partial t}+\nabla.(r_L\rho_L V_L)-S_{GL}=0 \quad (2)$$

Where S_{LG} is rate of mass transfer from liquid to gas phase and vice versa. Mass transfer between phases should balance local condition:

$S_{LG} = -S_{GL}$

Momentum conservation

Gas phase:

$$\frac{\partial(r_G\rho_G V_G)}{\partial t}+\nabla.(r_G(r_G\rho_G V_G))=$$
$$-r_G\nabla P_G+\nabla.\left(r_G\mu_{eff,G}\left(\nabla V_G+(\nabla V)^T\right)\right)+r_G\rho_G g-M_{GL} \quad (3)$$

Liquid phase:

$$\frac{\partial(r_L\rho_L V_L)}{\partial t}+\nabla.(r_L(r_L\rho_L V_L))=$$
$$-r_L\nabla P_L+\nabla.\left(r_L\mu_{eff,L}\left(\nabla V_L+(\nabla V)^T\right)\right)+r_L\rho_L g-M_{GL} \quad (4)$$

M_{GL} describes the interfacial forces acting on each phase due to presence of other phase.

Energy conservation

Gas Phase:

$$\frac{\partial(r_G\rho_G h_G)}{\partial t}+\nabla.(r_G\rho_G V_G h_G)=-\nabla.q+(Q_{LG}+S_{LG}h_{LG}) \quad (5)$$

Liquid Phase:

$$\frac{\partial(r_L\rho_L h_L)}{\partial t}+\nabla.(r_L\rho_L V_L h_L)=-\nabla.q+(Q_{LG}+S_{LG}h_{LG}) \quad (6)$$

h_L and h_G are specific enthalpies of given liquid and gas phase. The first term in the parentheses on the right hand side of above equations is energy transfer between phases, and the second term is the energy transfer associated with mass transfer between phases. Heat transfer between phases must satisfy local balance condition (Table 2):

Mass transfer equation: Transport equation for mass fraction of lighter component can be given as:

Gas phase:

$$\frac{\partial(r_G\rho_G Y_A)}{\partial t}+\nabla.\left[r_G\left(\rho_G V_G Y_A-\rho_G D_{AG}(\nabla Y_A)\right)\right]-S_{LG}=0 \quad (7)$$

Liquid phase:

$$\frac{\partial(r_L\rho_L Y_A)}{\partial t}+\nabla.\left[r_L\left(\rho_L V_L Y_A-\rho_L D_{AL}(\nabla Y_A)\right)\right]-S_{LG}=0 \quad (8)$$

Closure Models: The closure models are required for interphase transfer quantities, momentum, heat and mass transfer, and turbulent viscosities. The turbulence models are used to relate the mean flow variables. The k-epsilon model is used in this case the rate of energy transfer between phases can be:

$$Q_{LG}=\beta_{LG}a_e(T_L-T_G) \quad (9)$$

β_{LG} is a coefficient of heat transfer between phases. Suitable correlations of Nusselt number can be used to calculate Heat Transfer coefficient.

Volume conservation equation: This is simply the constraint that

the sum of volume fractions is unity.

$$R_L + R_G = 1 \tag{10}$$

Pressure constraint: The set of complete hydrodynamic equations represent 9 (4NP+1) equations in the 10 (5NP) unknowns U_L,$\mathbf{V_L}$, W_L, R_L, P_L, U_G, $\mathbf{V_G}$, W_G, R_G, P_G. We need one (NP-1) more equation to close the system. This is given by constraint on the pressure, namely that two phases share the same pressure field:

$$P_L = P_G = P \tag{11}$$

The drag correlation given by Krishna et al. [6], is a relation for the rise of a large bubbles in the turbulent regime given as:

$$C_D = \frac{4}{3}\frac{\rho_L - \rho_G}{\rho_L} g d_G \frac{1}{V^2_{SLIP}} \tag{12}$$

Where the slip velocity, $V_{SLIP} = |V_G - V_L|$, is estimated from the gas superficial velocity, **Vs**, and the average gas holdup fraction in the froth region.

$$V_{SLIP} = \frac{V_S}{R_G} \tag{13}$$

From the given equations the interphase momentum transfer term as a function of local variables becomes:

$$M_{GL} = \frac{R_G}{(1-R_G)V^2_S} g(P_L - P_G) R_G R_L |V_G - V_L|(V_G - V_L) \tag{14}$$

From the above relation it can be clearly seen that interphase momentum transfer is independent of bubble diameter, and is suitable for CFD use. The available data from the literature gives the average values of mass transfer coefficient and is not suitable for calculation in CFD simulations of mass transfer on sieve tray.

Outline condition

The liquid and vapour-outlet boundaries were specified as mass flow boundaries with fractional mass flux specifications. At the liquid outlet, only liquid was assumed to leave the flow geometry and only gas was assumed to exit through the vapour outlet. These specifications are in agreement with the literature, where only one fluid was assumed to enter [3]. A no-slip wall boundary condition was specified for the liquid phase and a free slip wall boundary condition was used for the gas phase. Initially only liquid fills the region between trays and vapour enters from holes at the bottom tray.

Simulations were conducted using single processor (2.4 GHZ). CFD analysis was carried on FLUENT 6.3 package of Ansys, Inc and Ansys 12.01. The solution procedure is based on the finite-volume method. The whole tray space, from liquid inlet to the outlet weir is considered in computational domain, even though the primary focus is on the froth section. This resulted in a better numerical convergence as well as providing us the ability to assess the froth height from the simulations. A time step of 0.001 seconds is used for simulations. The efficiency and clear liquid height is calculated after the steady state is achieved. This resulted in a better numerical convergence as well as providing us with the ability to assess the froth height from the simulations. Hydraulic parameters such as clear-liquid height and froth height were calculated at each time step. Runs continued until quasi-steady-state has reached, in other words, a simulation was deemed to have converged whenever the clear liquid height value reached a value no appreciable change in successive time steps. Although many of the simulations were inherently transient, an averaged quantity like the clear-liquid height appears to have reached a steady value; this criterion was used to terminate a simulation even if local values were changing in successive time steps in a bounded, chaotic manner. Several runs were taken as low as 5 weeks CPU time to be completed.

From drag coefficient term (eq. 12 in this work), at a given gas flow rate the use of the Bennet et al. [1] correlation amounts to using a constant multiplier as a drag coefficient. This constant factor is inversely proportional to the average liquid holdup fraction, but it is proportional to the second power of the average gas holdup fraction. Over predicting the average liquid holdup fraction results in a reduction in the interphase drag term (Table 3). The gas then does not exert enough drag force on the liquid. This can be thought of as if the tray were operating at a slightly lower gas rate than the actual one, which results in a larger clear-liquid height. However, these interpretations are not satisfactory. Use of governing equations, derived based on the assumption of a single bubble size, generally lead to significant over prediction of gas volume fraction, though comparison of liquid phase mean velocity is not bad.

Simulations

Specification	Rectangular Tray	Circular Tray
Length*width*height	260*233*233	
Height of weir	60mm	60mm
Height of Tray	233mm	233mm
Distance between inlet and outlet	260mm	260mm
Length of weir	233mm	233mm
No. of. holes	60	55
Diameter of holes	5mm	5mm
Triangular pitch	28mm	28mm
Inlet height	40mm	40mm
Ratio of hole area to bubbling area	0.0227	0.0227

Table 2: Specifications of rectangular and circular sieve tray.

Liquid inlet	Velocity inlet	Mixture	Temperature =333K
		Phase 1	Velocity=.001527 C6h6(l)=.4588
		Phase 2	Velocity=0 C6h6=0 Volume fraction=0
Liquid outlet	Pressure outlet	Mixture	Temperature =335K
		Phase 1	C6h6(l)=.4
		Phase 2	C6h6=0
vapour inlet	Velocity inlet	Mixture	Temperature =375K
		Phase 1	Velocity=0 C6h6(l)=0
		Phase 2	Velocity=0.567 C6h6=0.3138 Volume fraction=0.3508
vapour outlet	Pressure outlet	Mixture	Temperature =365K Gauge pressure = -25Pa
		Phase 1	C6h6(l)=0
		Phase 2	Velocity=0 C6h6=0.6896

Table 3: Boundary conditions for mixture and both liquid and vapour phase.

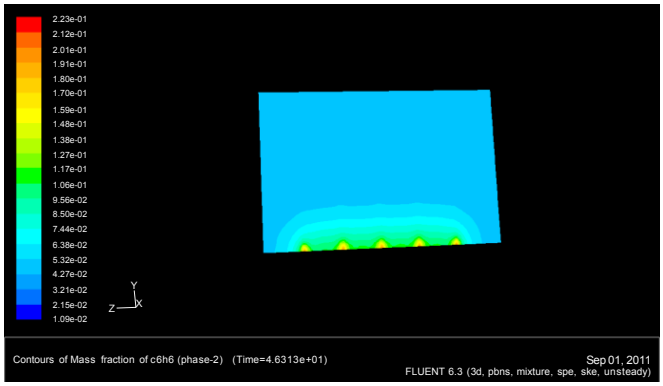

Figure 3: Mass fraction of benzene (gas phase).

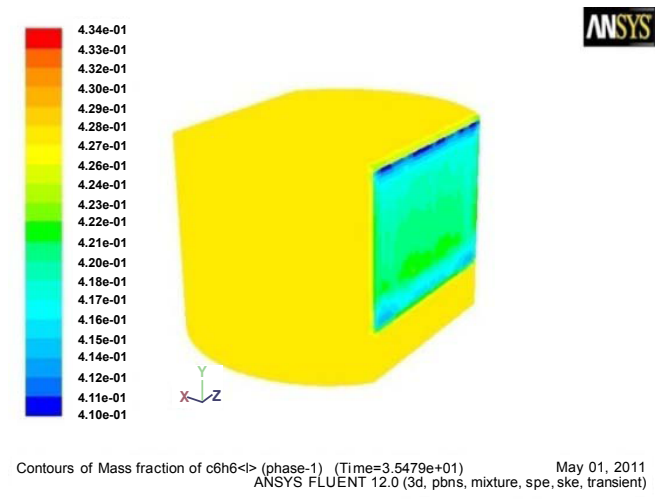

Figure 4: Mass Fraction benzene liquid between trays.

Circular sieve tray and rectangular sieve tray is created and put under simulations considering the inlet vapour liquid equilibrium for petroleum feedstock e.g. benzene-toluene mixture. Hydrodynamics, mass transfer and heat transfer is incorporated in the same hydrodynamics of sieve tray includes variation in mixture density, vapour velocity profiles and pressure profiles. Simulations were carried using time step of 0.001 seconds initially. Under-Relaxation factors were used for Energy, species and pressure conditions and simulations are initialized from liquid inlet [6,8,9]. Seven monitors were studied i.e. Velocity magnitude, Y-velocity, Static temperature, Density, Mass fraction of benzene and toluene liquid and volume fraction. Typically steady state is achieved in 51 seconds.

Results and Discussions

As expected the mass fraction of benzene in vapour phase is increasing and that in liquid phase is decreasing (Figure 5). This is due the more volatility of benzene as compared to the toluene. The pressure near the weir is very high as compared to that of liquid inlet. This may be due to liquid load towards the weir (Figure 3). Pressure drop is observed on moving from bottom plate to top plate. Initially the whole region is filled with liquid. As the vapour and liquid comes in contact, it is observed that vapour is occupying the region above the weir and variation in density can be seen from density profile .Velocity of vapour near the top plate is increasing.

Composition Profile

Clear liquid height was calculated against the simulated results using Bennet et al. [1] correlation and walis correlation. The results are fairly matching with the simulated results with little error. The predicted clear liquid height, peclet number and vapour liquid residence time are estimated over the plate and contours obtained are shown in Figures 4 and Figure 5 for benzene in gas phase and liquid phase. The peclet number near 3 shows plug flow conditions. Liquid mixing decreases with increase in velocity [9].

Density and Pressure Profiles

From the Figure 5, it can be seen that on the bottom plate density is much higher due to more amount of liquid over bottom plate. As the distance from the bottom plate increases the vapour composition increases and density decreases. Pressure gradient can be seen in Figure 6 that causes liquid to flow over plate as can also be verified from literature. Pressure increases from vacuum and reaches steady state value of atmospheric pressure at height 10 mm above bottom sieve tray. At middle of the tray spacing pressure first increases sharply for first 9 seconds and then decreases to a steady state value of atmospheric pressure. At a height 10 mm below the top tray, pressure shows an abrupt behaviour. It can be seen from these graphs that pressure drop

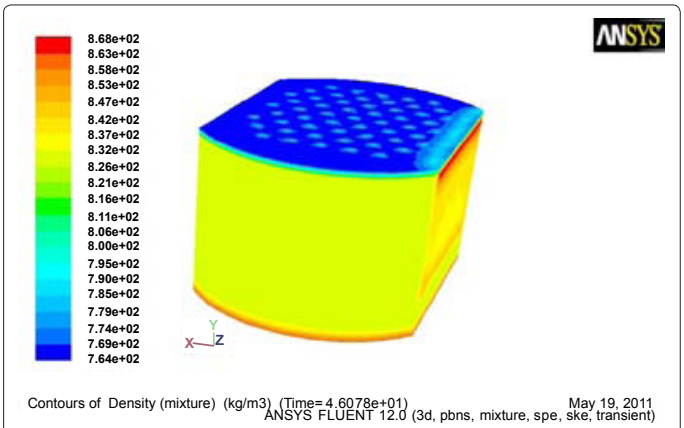

Figure 5: Density Profile.

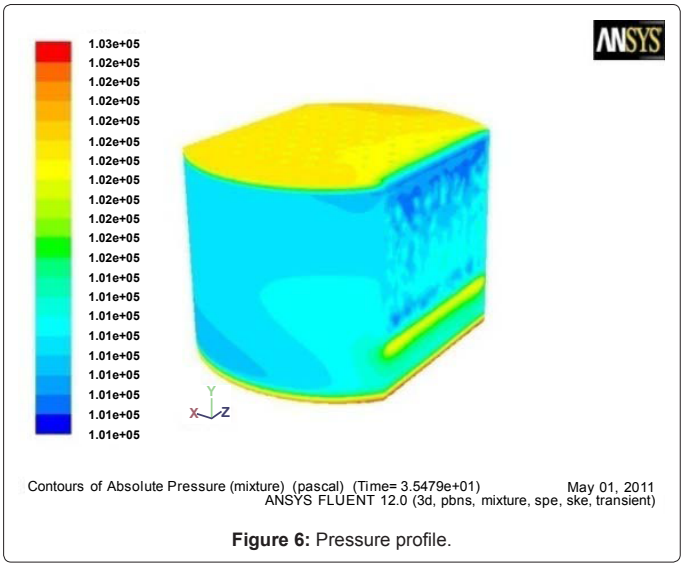

Figure 6: Pressure profile.

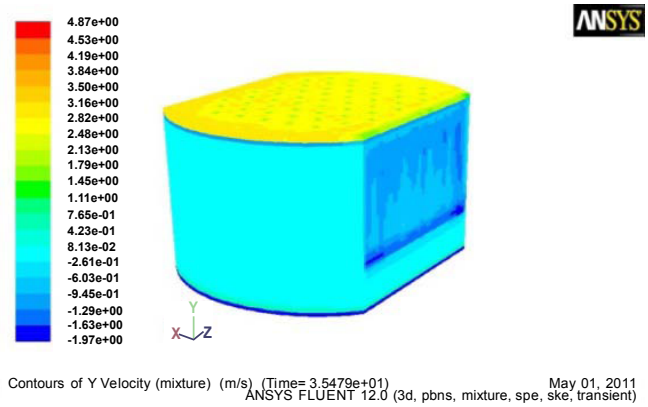

Figure 7: Y-Velocity Profile.

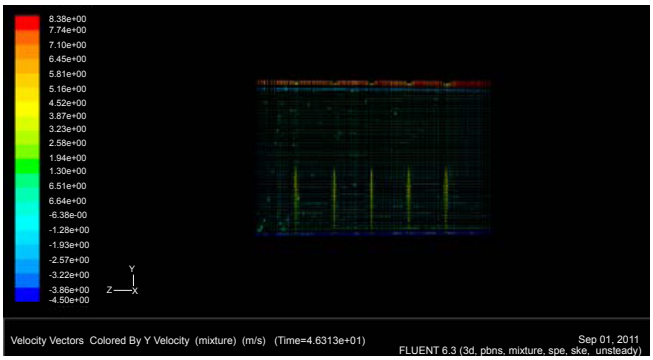

Figure 8: Velocity vectors.

S.No	Basis	Case I (velocity= 0.567m/s)	Case II(velocity =0.2835m/s)	Effect
1	Time to reach steady state	5 months	5 months	Almost same
2	Clear liquid height	71.03 mm	71.23 mm	Increased
3	Error in simulated results and correlation from Walis for clear liquid height	11.62%	7%	Decreased
4	Peclet Number	1.11	2.865	Liquid mixing decreases
5	Point efficiency	78.3%	82.17%	As vapor velocity is decreased, point efficiency is increased

Table 4: Tabulated Results.

occurs from bottom to top tray.

Velocity Profile

The Profile along the vertical direction over the plane is critically analyzed and contours for velocity is obtained as in Figure7. The Y-velocity, as can be seen in Figure 8, is higher close to top plate due to more vapour composition. The results for bottom tray were clearly shown that the gas flow rate distribution is non uniform along the tray, because of existence of hydraulic gradient and effect of relatively high residual pressure drop (Figure 9).

Comparison

A tabulated result (Table 4) is generated for two vapour velocities and various parameters are compared which plays critical role during distillation process. Murphree point Efficiency is calculated using correlation from literature [10] and compared for two different velocities and with increase in velocity the efficiency decreases while clear liquid height remains almost same. The clear liquid height first decreases with time and then reached to steady state value of 71.03 mm.

Conclusions

This study has shown that CFD can be used as a powerful tool for sieve tray design, simulation, visualization and troubleshooting. By means of CFD a virtual experiment can be developed to evaluate the tray performance .This study is a basis for development of new approaches for calculation of point and Murphree tray efficiencies. It can offer a great help in enhancing the efficiency of distillation tray column by varying design parameters such as weir height, down comer clearance, hole size, etc or the operating conditions like temperature, pressure, inlet vapour velocity and liquid weir load for different multi component systems. Also it can be used to find the best suited tray in terms of efficiency, pressure drop, capacity, etc. out of three conventional trays i.e. sieve tray, bubble cap tray and valve tray [11-14]. Although distillation is generally recognized as one of the best developed chemical processing technologies there are still many technical barriers, mainly related to equipment performance, that could, when overcome, secure the position of the distillation and even make it more attractive for use in future.

References

1. Bennett DL, Agrawal R, Cook PJ, (1983) New pressure drop correlation for sieve tray distillation columns. AIChE J 29: 434- 442.
2. Liu CJX, Yuan G, Yu KT, Zhu XJ (2000) A fluid-dynamic model for flow pattern on a distillation tray. Chemical Engineering Science 55: 2287-2294.
3. Doherty MF, Malone MF (2001) Conceptual Design of Distillation Systems. McGraw Hill Book Company Inc, New York.
4. Gesit GK, Nandakumar K, Chuang KT (2003) CFD modeling of flow patterns and hydraulics of commercial-scale sieve trays. AIChE J 49: 910-924.
5. Hughmark GA (1971) Models for Vapour-phase and Liquid phase Mass Transfer on Distillation Trays. AIChE J 17: 1295-1299.
6. Krishna R, Urseanu MI, Van Baten JM, Ellenberger J (1999) Rise Velocity of a Swarm of Large Gas Bubbles in Liquids. Chemical Engineering Science 54: 171-183.
7. Marshall WR (1954) Atomization and Spray Drying. Chemical engineering progress monograph 50: 87.
8. http://home.shirazu.ac.ir/~eor/cvfiles/absvafaei.pdf
9. http://www.iaeng.org/publication/WCECS2007/
10. Rahimi MR (2005) CFD Simulation of Hydrodynamics and Mass Transfer of Sieve Tray Distillation Columns. Ph. D. dissertation in chemical engineering, Sistan and Baluchistan University, Iran.
11. Stichlmair J (1988) Distillation and Rectification. Ullmann's Encyclopedia of Industrial Chemistry, Wiley.
12. van Houwelingen AJ, Sandrock C, Nicol W (2006) Particle wetting distribution in trickle-bed reactors. AIChE 52: 3532–3542.
13. http://doc.utwente.nl/58021/1/thesis_D_Zhang.pdf
14. Zuiderweg FJ (1982) Sieve trays: A view on the state of the art. Chemical Engineering Science 37: 1441-1464.